NASA Contractor Report 4477

A Comparison of Superconductor and Manganin Technology for Electronic Links Used in Space Mission Applications

R. Caton, R. Selim,
and A. M. Buoncristiani
Christopher Newport University
Newport News, Virginia

Prepared for
Langley Research Center
under Grant NAG1-1242

National Aeronautics and
Space Administration
Office of Management
Scientific and Technical
Information Program
1993

A Comparison of Superconductor and Manganin Technology for Electronic Links used in Space Mission Applications

R. Caton, R. Selim, and A.M. Buoncristiani

Christopher Newport College

Newport News, VA 23606

Funding Center: NASA Langley Research Center

Grant: NAG-1-1242

ABSTRACT

The electronic link connecting cryogenically cooled radiation detectors to data-acquisition and signal-processing electronics at higher temperatures contributes significantly to the total heat load on spacecraft cooling systems that use combined mechanical and cryogenic liquid cooling. Using high transition temperature superconductors for this link has been proposed to increase the lifetime of space missions. In this paper, we examine several YBCO ($YBa_2Cu_3O_7$) superconductor-substrate combinations and compare total heat loads to manganin wire technology in current use. Using numerical solutions to the heat-flow equations we demonstrate that replacing manganin technology with YBCO thick film technology can extend a seven year mission by up to one year.

Key words: high temperature superconductor, high T_c superconductor, space application, heat load, thermal conductivity, thick film

Abbreviations used in text:

YBCO	$YBa_2Cu_3O_7$
IR	infrared
SAFIRE	Spectroscopy of the Atmosphere Using Far Infra-red Emission
SIRTF	Space Infrared Telescope Facility
AWG	American wire gauge
YSZ	Y_2O_3-stabilized ZrO_2

Symbols used in the text:

A	cross-sectional area of link
c	2 heat
H_{30}	heat load for upper temperature of link at 30 K
H_{80}	heat load for upper temperature of link at 80 K
i	electric current
J	electric current density
K	thermal conductivity
L	length of link
R	electrical resistance
S	electrical power dissipated per volume
t	time
T	temperature
T_c	superconducting transition temperature
T_H	temperature of link at hotter end
T_L	temperature of link at cooler end
x	position
ρ	mass density
ρ_{elect}	electrical resistivity

I. Introduction

The discovery of a new class of ceramic superconductors with transition temperatures above the boiling point of liquid nitrogen has opened the doors for several important space applications. One near term application is the fabrication of an electrically conducting and thermally isolating link to replace manganin wires used in connecting IR detectors to data acquisition electronics on remote sensing platforms like SAFIRE and SIRTF. The SAFIRE mission employs hybrid dewars which combine both mechanical and cryogenic liquid cooling. This new technology is limited by the heat conducted through sensor array leads that connect the electronics (at ~ 80 K) to the sensors (at ~ 4 K). This link between a detector operating at 2-4 K and electronics operating at 30 - 80 K must be made of material that has high electrical conductivity and high thermal resistance. The YBCO superconductor with a transition temperature,T_c, of 93 K can achieve these conflicting requirements. A link with these characteristics will improve the thermal isolation of IR detectors and will increase the lifetime of the cryogen. A reduction of the thermal load due to the link by a factor of 4 will increase the lifetime of a 7 year mission by about one year. This report considers some of the principles that need to be addressed in order to develop a high T_c superconducting link for use in IR remote sensing platforms.

Using SAFIRE as an example of a cryogenically cooled remote sensing atmospheric mission that requires an electrically conducting and thermally isolating link connecting a detector at 4 K to electronics at 80 K, we note the following differences between conventional and superconducting links:

1. The state-of-the-art technology of conventional wires uses 158 manganin wires encased in Kapton ribbon. These #40 AWG manganin wires are approximately 6 inches long, with a 0.1 mil shield. For SAFIRE this conventional link produces 33 % of the instrument heat load on the liquid cryogen.

2. The state-of-the-art superconducting thick film technology produces $YBa_2Cu_3O_x$ wires made by the screen printing process. Wires are 2-4 mils in width at a 2-4 mil spacing, and 30-40 micron in thickness with a reduced cross sectional area of 1000-2000 μm^2 per wire. Such wires are printed on MgO, Al_2O_3, or YSZ (Y_2O_3-stabilized ZrO_2) substrates.

Using such high T_c material can result in a significant reduction of the heat load from the link. In this report we have investigated the effect of different parameters on the performance of the link: wire material, cross sectional area per wire, substrate material, and the thickness of the substrate. The studies have been done for two probable cases where the low temperature detector is at 4.2 K with the high temperature electronics at either 30 or 80 K.

II. Theory

We need to describe the heat transport in one dimension between two isolated thermal reservoirs, one at a high temperature T_H and and the other at a lower temperature T_L, linked by an element which has a thermal conductivity K and an electrical resistivity ρ_{elect} as shown in Figure 1. Heat flows from the high temperature reservoir to the low temperature reservoir and, in addition, when an electrical current flows through the element, heat is generated along its length. The local thermal energy density is given by the expression ρcT, where ρ is the mass density of the element, c is its specific heat capacity and T is its temperature. The rate at which this energy density changes is given by the thermal continuity equation

$$\frac{\partial}{\partial t}(\rho cT) = -\nabla \cdot \mathbf{J} + S .$$

Here $\mathbf{J}$ is the thermal flux vector, given by Fourier's law as, $\mathbf{J} = -K\nabla T$, and S is the local heat source. We assume that S is due to i^2R heating from the electrical conduction; that is

$$S = \frac{\text{Electrical Power Dissipated}}{\text{Volume}} = \frac{i^2R}{AL} = J^2 \rho_{elect} ,$$

where the cross-sectional area and length of the link are A and L, respectively. Assuming that the heat flow occurs only in the direction of the linking element we obtain the heat flow equation

$$\frac{\partial}{\partial t}(\rho cT) - \frac{\partial}{\partial x}\left(K\frac{\partial T}{\partial x}\right) = J^2\rho_{elect} .$$

Of course, in this expression the specific heat c, the thermal conductivity K, and the electrical resistance ρ_{elect} are functions of temperature.

We are mainly interested in the steady state behavior of the linking system which is governed by the following ordinary differential equation

$$\frac{d}{dx}\left[K(T)\frac{dT}{dx}\right] = -J^2 \rho_{elect}(T) .$$

This equation is discussed in a paper by Hull [1].

It is instructive to solve this equation first assuming that the thermal conductivity and electrical resistivity do not change with temperature; in this case the exact solution has the form

$$T(x) = T_L + (T_H - T_L)\, x - \frac{J^2 \rho_{elec}}{2K} \left(x^2 - xL\right).$$

The first two terms give the linear behavior of the thermal gradient contribution while the third term gives the contribution from the the electrical power dissipation in the link. Any further contributions to the spatial dependence of the temperature distribution are due to changes in the thermal conductivity with temperature. When the thermal conductivity and electrical resistance vary with temperature we must employ numerical techniques to determine the temperature distribution in the wire.

III. Calculation

Numerical calculations for the one-dimensional heat transfer problem were carried out using a Runge-Kutta method with MathCAD™ [2]. We have used thermal conductivity data from the literature for the following materials: manganin [3], YBCO [1], tetragonal YSZ [4], cubic YSZ [5], and amorphous silica [6]. Electrical resistivity data for manganin were taken from reference 3. At low temperatures the thermal properties of the materials under consideration depend on temperature (see Fig. 2). The temperature dependencies for the electrical resistivity and thermal conductivity were approximated by linear or quadratic functions using the data in the above references. It was found that the Joule heating was insignificant at the low current densities (≤ 0.1 A/cm^2) required for the proposed applications. The temperature and temperature gradient at the low temperature end of the sample were input as parameters to the numerical solution of the second order differential heat transfer equation. The program was run repeatedly, choosing a new temperature gradient until the temperature at the high temperature end of the sample met the specified design value. The step size for numerical integration was continually decreased until the solution stabilized. Typically this occurred when the step size was about one thousandth of the total interval size.

The results of a typical solution (in this case #40 manganin wire) are plotted in Fig. 3. The heat load should be the same everywhere along a one dimensional wire which implies that the product of thermal conductivity and dT/dx (which is proportional to the heat load) should remain constant. The thermal conductivity increases monotonically with temperature for manganin while dT/dx (the slope in Fig. 3) decreases. Analysis shows that this product remains constant which provides a good check on the correctness of the solution.

IV. Results

Since the proposed missions have different values for the temperature of the electronics, we have included two cases in Table 1. In both cases the detector is in contact with a reservoir at 4.2 K

(liquid helium), but in one case the electronics are at 30 K with a link 3 inches long and in another they are at 80 K with a 6 inch link. We have labeled the heat loads (in μW) H_{30} and H_{80} for the two cases, respectively. For purposes of comparison it is instructive to consider the case where the thermal conductivity remains constant as a first order approximation. For this case the thermal conductivity is taken as an appropriate average of the temperature varying value. We have included results for the calculation done numerically as described above (columns 2 and 4 in Table 1) and the results assuming constant thermal conductivity K (columns 3 and 5 in Table 1). For the constant K results we simply picked a straight average of the thermal conductivity values at the highest and lowest temperatures.

Manganin wires coated with Kapton have already been used as a interconnect from a lower to a higher temperature in space flight [7], so Table 1 includes manganin for comparison. The thermal conductivity of Kapton is so low that it is not considered and it probably would be used in similar amounts for the proposed YBCO link. Thus, we list the heat load per wire for manganin and YBCO deposited on three different substrates: tetragonal YSZ, cubic YSZ, and amorphous silica (a-SiO_2). We call the combined heat load for YBCO on the three substrates total 1, total 2, and total 3, respectively. In determining the amount of substrate needed per wire, we have used a thick film size for YBCO of 1 mil thick by 4 mils wide and assumed a 4 mil spacing between each YBCO wire. The area of substrate required for each wire then becomes 8 mils wide times the substrate thickness.

There are two things to be noted in Table 1. First, the estimates of the individual heat loads assuming a constant K can vary considerably from the more careful numerical calculation (the constant K estimate is 36% low for H_{80} for YBCO). In some cases the estimate assuming constant K varies in the opposite direction as for H_{80} for amorphous silica where the estimate is too high by 8%. The estimates assuming constant K for the YSZ substrates are not close to the numerical values of heat load in any case. The magnitude and sign of the difference between the constant K estimate and numerical result depend on the detailed shape of the thermal conductivity *vs.* temperature curve. Thus one must be cautious in interpreting the results using a constant K since different averaging methods could yield different comparisons. Clearly the numerical calculation which includes the temperature dependence of K is necessary for a reliable estimate and comparison of the heat load for various cases.

Secondly, we want to compare manganin to the various YBCO-substrate combinations and compare only the more reliable numerical results. Considering the H_{80} case, we see that the heat load for manganin (#40 wire) is greater than total 3 (YBCO-amorphous silica), but the manganin heat load is less than for totals 1 and 2. The results are similar for the H_{30} case; however, the YBCO-substrate combination is relatively better for the H_{80} case because the substrate thermal conductivities level off at the higher temperatures (>50 K) whereas K for manganin continues to increase approximately linearly (see Fig. 2). We have chosen an amorphous silica substrate of

thickness 6 mils for these comparisons, although such substrates are not readily available off-the-shelf, because there should be no difficulty in producing the thinner substrates. On the other hand, the fine manganin wire chosen for comparison is very difficult to handle and smaller diameter wire is not available and would most likely be extremely intractable. Six inch long bundles of hundreds of ultra-fine manganin wires would be a nightmare. In contrast, the thick films of YBCO on substrates would be relatively easy to handle.

The table clearly shows that the largest contributor to the heat load for the YBCO-substrate combinations is the substrate. The film width for YBCO (which controls the substrate width per wire) and substrate thicknesses are values we feel very confident in with present technology. It should be quite possible to get the substrate area per wire down by a factor of 2 to 4 which would reduce the substrate heat load contribution by 2 to 4. This would make all YBCO-substrate combinations an improvement over manganin wires, especially the YBCO-amorphous silica combination. Projections for this case where the YBCO film width and spacing are reduced by a factor of 2 appear in Table 2. Now YBCO on any substrate represents an improvement over #40 manganin wire. The result for the YBCO-amorphous silica combination projects an increased mission lifetime of about one year for a seven year mission compared to using #40 manganin wire.

The three combinations mentioned must continue to be considered because they all have advantages. Even though the YSZ substrates contribute a higher heat load, they are superior in strength and it is relatively easy to lay down thick YBCO films of high quality on YSZ substrates.

Thus far we have discussed only superconducting films on insulating substrates. The problem of the relatively high thermal conductivity of the substrate could be bypassed with stand-alone superconducting materials. The new laser-heated, pedestal-grown superconducting fibers offer a very attractive alternative to YBCO deposited on substrates [8]. High T_c superconducting fibers with diameters ranging from 40 to 90 microns have been produced. Links fabricated from these fibers would have contributions to the heat load comparable to YBCO alone which would result in a considerable improvement over manganin leads. This relatively new technology merits serious consideration.

A final comment is in order. Although the numerical calculations include a Joule heating term, the results for manganin (the only normal conductor) were not affected by the Joule heating term because the current for the envisioned application is quite low (1 μA). As the cross section of the manganin decreases or the electrical current increases, the Joule heating will increase. Our numerical calculations show that the Joule heating will begin to play a role to increase the heat load as the current approaches 100 μA for #40 manganin wire. This will occur sooner for #42 manganin wire because of its smaller cross-sectional area. For higher current applications the YBCO-substrate combinations will result in lower heat loads up to the point where the critical current is exceeded (≈ 5 mA assuming currently obtainable YBCO with a critical current density of

200 A/cm^2). At this point we would require better quality thick films of YBCO. A detailed analysis for heat transfer in the presence of large currents has been carried out by J. R. Hull [1].

V. Conclusion

We have carried out an analysis of the heat load on a cooling system using low-temperature detectors. This analysis shows the importance of using the numerical solution to the differential equations for one-dimensional heat flow in estimating the heat load of interconnects in planned space flight missions. Simply assuming an averaged constant value for the thermal conductivity to estimate the heat load can lead to considerable error. With current technology the YBCO-substrate combinations result in numerically calculated heat flows comparable to those for available manganin wires. While there is little chance of reducing the heat load contribution using manganin wires, there is a good chance of obtaining considerable reduction using a YBCO-substrate combination or using superconducting fibers. Superconductors should continue to be explored as low-current carrying interconnects for missions where the interconnect contribution to the heat load plays a predominant role in the lifetime of the mission. As the number of interconnects increases, the thick film superconducting links or superconducting fibers will be more attractive.

ACKNOWLEDGEMENT

We wish to acknowledge NASA for their support of this work with Grant NAG-1-1242. We would like to thank Stephanie Wise, Matthew Hooker, and Ira Nolt for helpful discussions.

REFERENCES

1. J. R. Hull, *High temperature superconducting current leads for cryogenic apparatus*, Cryogenics **29**, 116 (1989).
2. Mathsoft, Inc., *MathCAD$^{2.0}$* (MathSoft, Inc., Cambridge MA, 1987).
3. M. Fogiel, *Handbook of Mathematical, Scientific, and Engineering Formulas, Tables, Functions, Graphs, Transforms*, p. 799 (Research and Education Association, New York, NY, 1986)
4. W. N. Lawless and T. K. Gupta, *Thermal properties of tetragonal ZrO_2 at low temperatures*, Phys. Rev. **B 28**, 5507 (1983).
5. D. A. Ackerman, D. Moy, R. C. Potter, and A. C. Anderson, *Glassy behavior of crystalline solids at low temperatures*, Phys. Rev. **B 23**, 3886 (1981).
6. Thermal Conductivity Measurements of Insulating Materials at Cryogenic Temperatures, a

Symposium, Philadelphia, American Society for Testing and Materials (1967).
7. An ORBIT Engineering Performance Review / COBE, Goddard Space Flight Center, March 7-8, 1990.
8. R. S. Feigelson, *Pulling optical fibers*, J. of Crystal Growth **79**, 669 (1986). R. S. Feigelson, D. Gazit, D. K. Fork, and T. H. Geballe, *Superconducting Bi-Ca-Sr-Cu-O fibers grown by the laser heated pedestal growth method*, Science **240**, 1642 (1988).

Table 1: Comparison of heat flows in μW for various materials and cases.

Material	H_{30} numerical calculation	H_{30} constant K calculation	H_{80} numerical calculation	H_{80} constant K calculation
Manganin #40	4.6	4.6	16.6	15.4
$YBa_2Cu_3O_7$ *	1.0	1.0	2.5	1.6
YSZ tetragonal **	11.2	9.3	25	16
Total 1	12.2		27.5	
$YBa_2Cu_3O_7$ *	1.0	1.0	2.5	1.6
YSZ cubic **	7.4	6.0	17	13
Total 2	8.4		19.5	
$YBa_2Cu_3O_7$ *	1.0	1.0	2.5	1.6
a-SiO_2 **	1.6	1.6	4.6	4.9
Total 3	2.6		7.1	

* Assuming 1 mil x 4 mil films

** Assuming a 6 mil thick substrate

Table 2: Comparison of heat flows in μW for a 2 mil spacing.

Material	H_{80} numerical calculation
Manganin #40	16.6
$YBa_2Cu_3O_7$ *	1.3
YSZ tetragonal **	12.5
Total 1	13.8
$YBa_2Cu_3O_7$ *	1.3
YSZ cubic **	8.5
Total 2	9.8
$YBa_2Cu_3O_7$ *	1.3
a-SiO_2 **	2.3
Total 3	3.6

* Assuming 1 mil x 2 mil films

** Assuming a 6 mil thick substrate

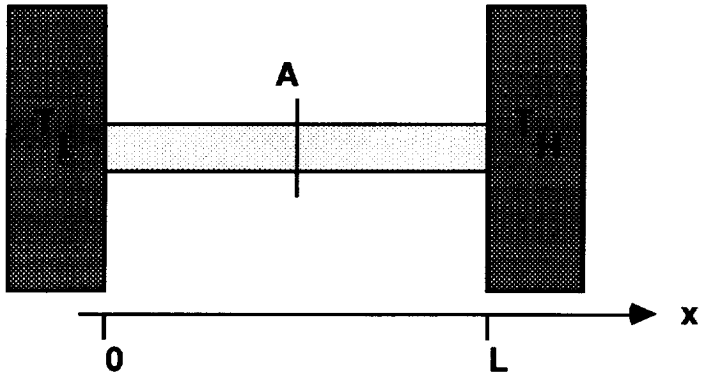

Figure 1. Schematic diagram of the link with important parameters indicated: TL - temperature of the lower temperature reservoir (detector) TH -temperature of the higher temperature reservoir (electronics) A - cross-sectional area of the link, and L - length of the link.

Figure 2. Thermal conductivity vs temperature for various materials

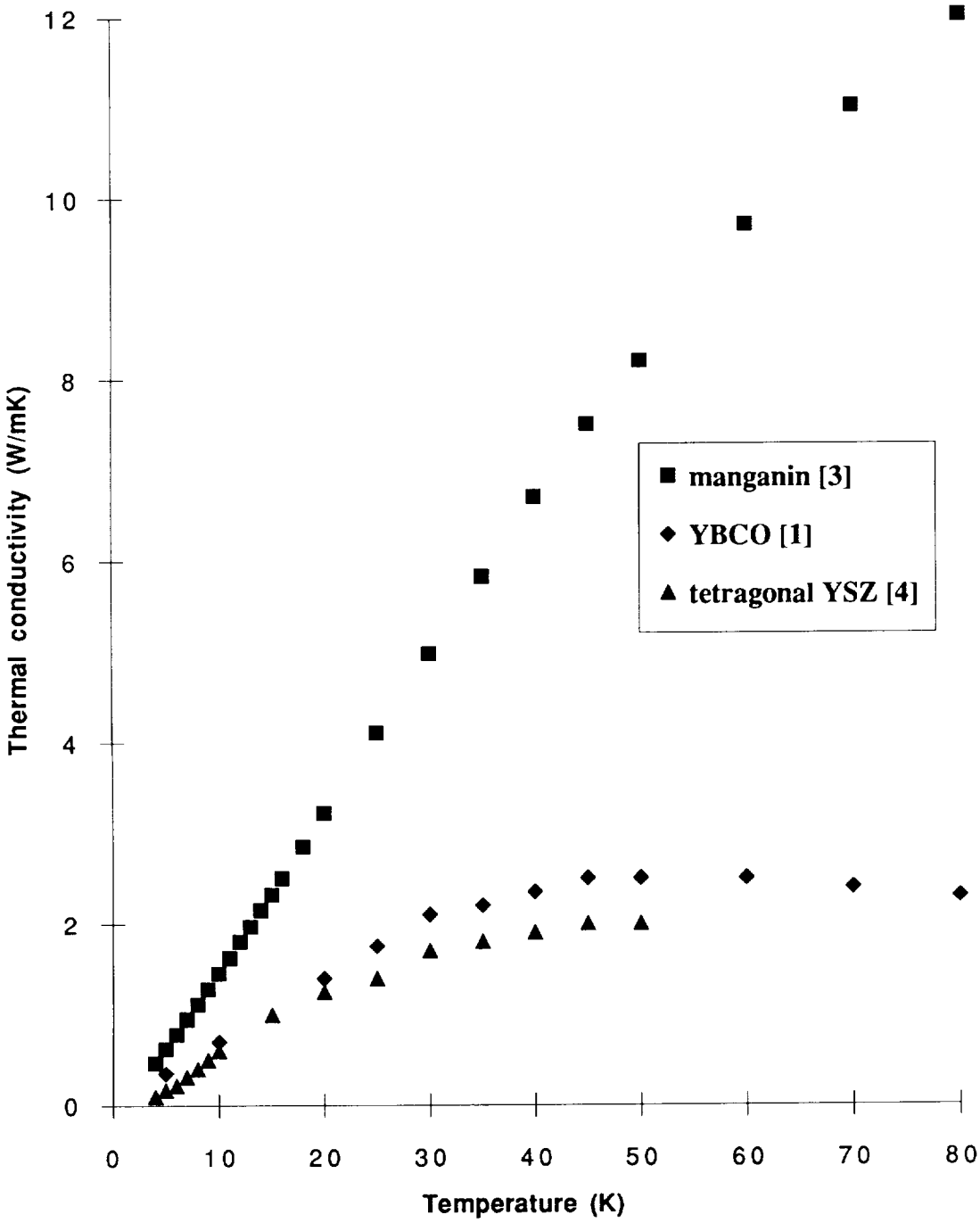

Figure 3. Temperature along the link vs position along the link for the numerical calculation of the case where TL = 4.2 K and TH = 80 K for #40 manganin wire.